

Social reinforcement with weighted interactionsThéo Konc^{1,*} and Ivan Savin^{1,2}¹*Institute of Environmental Science and Technology, Universitat Autònoma de Barcelona, Spain*²*Graduate School of Economics and Management, Ural Federal University, Yekaterinburg, Russian Federation*

(Received 7 December 2018; revised manuscript received 3 May 2019; published 9 August 2019)

The speed and extent of diffusion of behaviors in social networks depends on network structure and individual preferences. The contribution of the present study is twofold. First, we introduce weighted interactions between potential adopters that depend on the similarity in their preferences and moderate the strength of social reinforcement. The reason for the extension is the existence of a confirmation bias in the way agents treat information by prioritizing evidence conforming to their opinion. As a result, individuals become less likely to be influenced by peers with relatively different preferences, reducing the overall diffusion rate under clustered networks. Second, we enrich our analysis by also considering a scale free network topology with a high degree asymmetry, motivated by its pervasiveness in online social networks. This network performs consistently well in terms of diffusion for different parameter combinations and clearly outperforms clustered networks under weighted interactions. Our results show that more realistic assumptions regarding agents' interactions shift the focus from clustering to degree distribution in the study of network structures allowing for fast and widespread behavior adoption.

DOI: [10.1103/PhysRevE.100.022305](https://doi.org/10.1103/PhysRevE.100.022305)**I. INTRODUCTION**

Individual decision making is sensitive to conspicuous peer behavior. This has been confirmed, among others, for energy consumption choices [1,2], adoption of solar panels [3], and greenhouse gas mitigation practices (including usage of public transport and recycling; see [4]). Social influence is often the result of descriptive norms, i.e., a regularity in the behavioral pattern of peers that signals a socially “correct” behavior [5]. The adoption of such behaviors is triggered by the percolation process—only those agents can adopt that are exposed to peers that already adopted the behavior—and by the social reinforcement process—every further peer increases the likelihood of adoption.

Many studies have modeled the diffusion of a behavior at the individual level in an explicit social network searching for a topology ensuring fast and widespread adoption [6,7]. The main topological features investigated are the average path length (average number of edges along the shortest path between any two nodes) and the clustering (the extent to which peers of any node tend to be also peers with each other) of the network [8]. Shorter average path length allows for a faster spreading of information. High clustering enhances a local diffusion via the social reinforcement process. The role of clustering has been demonstrated in an experiment by Centola [7], where participants faced the decision to join a health forum. Every time a participant registered to the forum, a message was sent to her social neighborhood inviting the recipients to join as well. This study found that participants were more likely to join as the number of invitations they received grew, demonstrating the role of social reinforcement.

Furthermore, exploring different network topologies Centola concluded that behaviors subject to social reinforcement diffuse at a higher rate in clustered networks. Several modeling studies reproduced this finding. Reference [9] builds a simple model of information diffusion where the likelihood of accepting and transmitting the information increases with the number of signals received. Reference [10] uses a threshold model, in which agents adopt a behavior depending on peer pressure and individual preferences are defined as intrinsic cost to adopt a new behavior.

We introduce two differences to the model by [10]. First, we consider that the peer pressure between two agents depends on the similarity in their preferences. Second, we include the scale free network topology in our analysis. Both differences are motivated by extensive empirical evidence documenting relevance of these assumptions. In particular, as demonstrated by [11], agents put a higher weight on opinions that conform to their existing beliefs, pointing out an important confirmation bias in the way agents treat information. Later the confirmation bias was demonstrated in different contexts [12–14], with experiments showing that agents are more likely to comply with a norm communicated by a peer with similar preferences [15]. To model the confirmation bias, we introduce weighted edges based on the distance in agents' preferences. In other words, the social influence one agent exerts on another is not binary (signal the behavior or not), but mediated by their similarity in preference towards adopting that behavior. Our conjecture is that this bias can affect the performance of the studied networks in terms of diffusion rates. Including the scale free network is motivated by the increasing empirical evidence that online networks exhibit the power law degree distribution [16,17], while interactions occur with ever greater extent online [18]. This particular topology is the result of the preferential attachment process

*theo.konc@uab.cat

where few nodes have a very large number of connections and the majority of nodes have very few peers only [19]. While simple diffusion in the scale free network has been studied in [20,21], this paper is addressing the scale free topology for complex diffusion with social reinforcement and weighted interactions.

We demonstrate that, first, the addition of insights from behavioral science on how agents asymmetrically treat information undermines the performance of clustered networks. This is because the long average paths between nodes in the network allow individuals to resist social pressure from peers with very different preferences precluding further spreading of the behavior. Second, we show that the scale free network is robust to the weighting of interactions. It best ensures fast and widespread diffusion under social reinforcement and confirmation bias when the majority of the population has a high resistance against adopting the behavior. These two results are important for the literature in understanding the complex processes of social diffusion shifting the focus from network clustering to network degree distribution as the critical factor for behavior spreading. They also suggest that the diffusion of a behavior is more effective on digital social platforms than on spatial offline networks where high degree asymmetry is less likely.

The remainder of this paper is organized as follows. Section II describes our model of diffusion with social reinforcement under confirmation bias. There we introduce weighted interactions and the scale free network topology not considered in this context earlier. Section III presents simulation results. Section IV concludes.

II. MODEL

A. Percolation with social reinforcement

We describe a simple model of behavior adoption with social reinforcement and confirmation bias, in which the decision to adopt is based on personal preferences, awareness about certain behavior (percolation model), and peer pressure. Following [10], we consider agents interacting in a fixed undirected social network N , where the set of agent i 's neighbors is denoted by N_i and its degree by n_i .¹ The agent decides to adopt the behavior if and only if

$$Q \geq m_{i,t}, \tag{1}$$

where $Q \in [0, 1]$ is the quality of the behavior and $m_{i,t}$ is the minimum quality requirement (or MQR) of agent i .² A zero quality means a completely unattractive behavior that no one is willing to adopt, while a quality of one means a behavior

¹Uppercase letters denote sets and the corresponding lowercase letters the cardinality of the respective sets.

²Quality is an abstract aggregate term. Referring to the examples from the Introduction, quality captures the effectiveness of measures mitigating greenhouse gas emissions or technical quality of solar panels. Instead of quality, one can also operate with prices: Q as a market price and MQR as a reservation price of the agent [22]. Considering the more expensive electricity from the renewable energy sources as a new behavior, social reinforcement raises the agent's willingness to pay and adopt the new behavior.

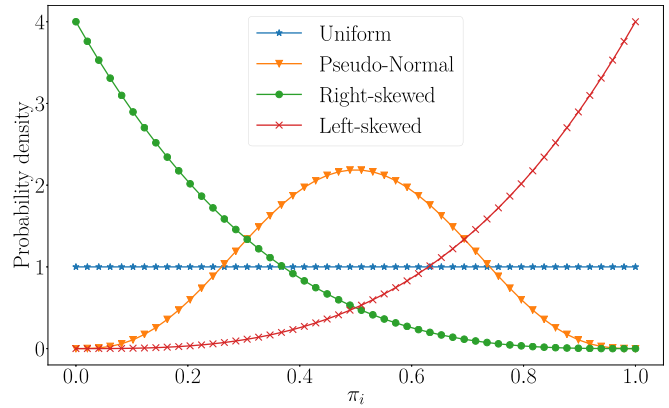


FIG. 1. Different distributions of switching costs (π_i).

that everybody wants to adopt from the moment they are informed about it. The minimum quality requirement without confirmation bias is a decreasing function of the number of adopting peers:

$$m_{i,t} = \pi_i(g_{i,t})^{-\gamma}, \tag{2}$$

with $\gamma \in [0, 1]$ capturing the intensity of social reinforcement in the decision making, $G_{i,t} \subseteq N_i$ being the subset of adopters among agent i 's peers at time t , $g_{i,t} \leq n_i$ being the number of adopters among agent i 's peers at time t , and $\pi_i \in [0, 1]$ being the intrinsic switching cost of agent i towards a given behavior. The switching costs are inversely related to intrinsic preferences in adopting the new behavior. An agent with high switching cost may adopt only if several peers influence her to do so. An agent with low switching costs will adopt as soon as one peer signals her the behavior. In the following, we will interchangeably refer to preferences and switching costs that both capture the individual resistance in adopting a certain behavior (MQR). Heterogeneous switching costs between agents can be explained by differences in income, education, environmental concern, available infrastructure, and even amount of free time to adopt the new behavior.³ In line with [10], we assume that switching costs between neighbors are independent. This means that the generating process of the network is unrelated to the particular behavior in question. The preferences follow a Beta distribution: $\pi_i \sim B(\beta_1, \beta_2)$. This distribution family is flexible, allowing us to study several settings (Fig. 1) as follows.

- (i) A uniform distribution with $\beta_1 = 1, \beta_2 = 1$.
- (ii) A pseudonormal distribution with $\beta_1 = 4, \beta_2 = 4$.
- (iii) A right skewed distribution (the majority of agents have strong preference for the behavior) with $\beta_1 = 1, \beta_2 = 4$.
- (iv) A left skewed distribution (the majority of agents have strong preference against the behavior) with $\beta_1 = 4, \beta_2 = 1$.

In the rest of the paper, we will focus on the results for the latter specification of the Beta distribution [π_i drawn for the $B(4, 1)$ with the majority of people having high switching costs]. This setting corresponds best to the case where social

³Consider, for example, the choice to adopt waste sorting behavior where the above-mentioned characteristics can serve as arguments in favor of or against adopting the new norm.

reinforcement makes a difference with many agents adopting because of social pressure [10].⁴

While network position (and the resulting number of adopters in the neighborhood) and switching costs are heterogeneous across agents, other parameters, like the intensity of social reinforcement and behavior quality, act uniformly for all agents.

B. Weighted interactions and confirmation bias

The first difference of our approach is to differentiate the influence of peers on the agent's decision to adopt depending on the distance in their preferences. In doing so, we follow the literature on the confirmation bias showing that opinion dynamics between two agents depends on their opinion proximity [23–25]. The bias arises due to often unconscious selectivity in searching, interpreting, and remembering evidence supporting one's own opinion. In this framework, agents assign more weight to opinions that already conform to their beliefs, while “neglecting to gather, or discounting, evidence that would tell against it” [13, p. 175]. While [26] captures this bias by allowing agents to regard only those peers who are sufficiently close in their opinion, we follow [27] by allowing agents being both close and far in their intrinsic preference to affect their peers' decision but with different weights. For instance, observing someone having the same preference adopting certain behavior is more persuasive than observing someone with a very distant preference. By doing this, we introduce heterogeneity in terms of peer pressure the agent can experience from different neighbors. Also, we extend the social interaction process underlying our model. While in [10] it was only about sharing information about adoption decision (“showing”), here we assume agents know and differentiate between preferences of their peers (i.e., “telling” information about the reasons behind their adoption) [28].

We proceed by extending MQR with the confirmation bias as follows:

$$m_{i,t} = \pi_i \left(\frac{\sum_{j \in G_{i,t}} e^{-\rho|\pi_i - \pi_j|}}{\sum_{k \in N_i} e^{-\rho|\pi_i - \pi_k|}} n_i \right)^{-\gamma}, \quad (3)$$

with $\rho \in [0, +\infty)$ being the strength of confirmation bias, N_i being the set of peers of agent i , $G_{i,t} \subseteq N_i$ being its subset that adopted the behavior at time t , and n_i being the degree of agent i . The strength of the signal flowing from agent j to agent i is $e^{-\rho|\pi_i - \pi_j|}$. The ratio in Eq. (3) represents the relative weight of the signal from the adopting peers. We multiply this ratio by the agent's degree n_i so that Eq. (2) without confirmation bias proposed by [10] can be seen as a special case of our Eq. (3) with $\rho = 0$. Furthermore, MQR of agent i would be the same in both models if agent i is surrounded by agents with the same preference [Eq. (4)]:

$$m_{i,t} = \pi_i \left(\frac{g_{i,t}}{n_i} n_i \right)^{-\gamma} = \pi_i (g_{i,t})^{-\gamma} \quad \text{if } \forall \pi_k = \pi_i \quad (4)$$

or if all peers of agent i adopted the behavior [Eq. (5)]

$$m_{i,t} = \pi_i (1 \times g_{i,t})^{-\gamma} \quad \text{if } g_{i,t} = n_i. \quad (5)$$

TABLE I. Network characteristics for 10 000 nodes and 20 000 undirected links. (*Note.* Average clustering is measured as an average probability for every node that any two of her neighbors are connected. Average path length measures the average number of links required to connect two nodes. Degree asymmetry of a network is measured by the skewness of its degree distribution.)

	Average clustering	Average path length	Degree asymmetry
Regular lattice	50.00%	1250.00	0.00
Small world	35.62%	12.50	0.12
Random	0.04%	6.76	0.50
Scale free	0.15%	4.27	36.30

Thus, introducing the confirmation bias, we effectively transform our network from an unweighted to a weighted one.

Note that MQR with confirmation bias from Eq. (3) being a function $f(\pi_i, g_{i,t}, \gamma)$ can exceed the original switching cost π_i if the distance in switching costs to the adopters in agent i 's neighborhood is larger than the average distance to all his neighbors:

$$\sum_{j \in G_{i,t}} e^{-\rho|\pi_i - \pi_j|} \leq \frac{\sum_{k \in N_i} e^{-\rho|\pi_i - \pi_k|}}{n_i}. \quad (6)$$

That means $f(\pi_i, 1, \gamma) = \pi_i$ does not always hold anymore (unlike in [10]), but f can be larger or smaller than π_i depending on the distance in preference to the first adopting peer.⁵ One should, however, not mix it with a possible deterring effect in our model since π_i is only an ingredient of MQR. In line with the fundamental principle of a percolation model, $f(\pi_i, 0, \gamma) = \infty$ (an agent cannot adopt a behavior if she is not aware of it), and $f(\pi_i, g_{i,t}, \gamma)$ is strictly decreasing in $g_{i,t}$ for $\gamma > 0$.

For very large ρ , the agents only consider the decision of their most similar neighbors. Let us consider the case when agent l is the most similar (in terms of preference) peer of agent i , i.e., $|\pi_i - \pi_l| < |\pi_i - \pi_k| \forall k \neq l \in N_i$. Then:

$$\lim_{\rho \rightarrow \infty} e^{-\rho|\pi_i - \pi_j|} = 0 \quad \forall j \in N_i \quad (7)$$

and

$$\lim_{\rho \rightarrow \infty} (e^{-\rho|\pi_i - \pi_l|} + e^{-\rho|\pi_i - \pi_k|}) = e^{-\rho|\pi_i - \pi_l|}. \quad (8)$$

Therefore, for the strength of the confirmation bias approaching infinity, we have agents simplifying the behavior of their whole ego network to the behavior of their closest peer:

$$m_{i,t} = \begin{cases} \pi_i (n_i)^{-\gamma} & \text{if } l \in G_{i,t}, \\ 0 & \text{else.} \end{cases} \quad (9)$$

C. Network topology

Our second difference is that we extend the set of networks considered with the scale free network. The reason is that many empirical networks present a very high degree asymmetry. This holds particularly true for digital social networks due

⁴The results for other distributions can be found in Appendix C.

⁵The inequality in Eq. (6) can hold even for two or more adopting peers.

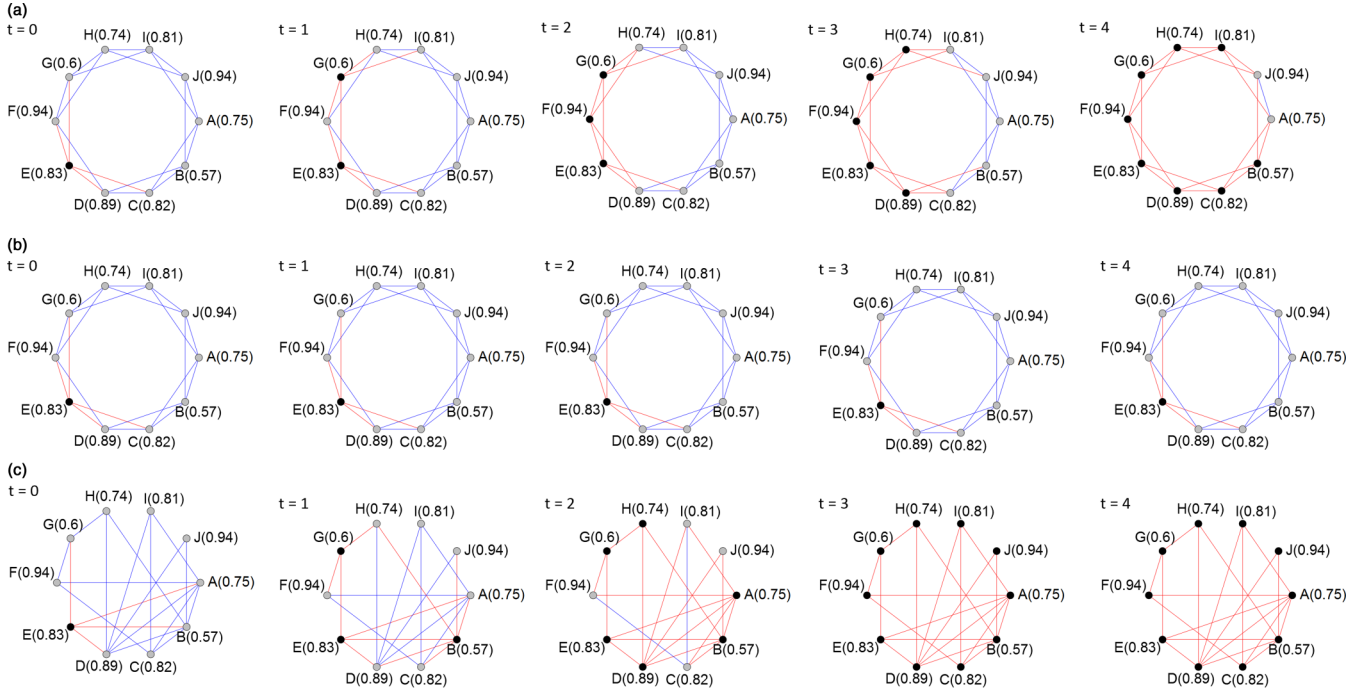


FIG. 2. Example of a diffusion process for $Q = 0.6$, $\gamma = 1$, and $B(4, 1)$ in (a) a regular lattice without confirmation bias, (b) a regular lattice with confirmation bias, $\rho = 1$, and (c) a network with high degree asymmetry with and without confirmation bias. *Note.* Scalars in parentheses are the switching costs of each agent. Black nodes represent agents having adopted the behavior, while gray nodes are agents that are subject to adopt; red links represent the signal flowing from the adopting agent to its neighbors.

to the lower time constraint associated with maintaining on-line communication allowing agents to have a very large number of connections [17]. As a result, few star agents can have a high number of peers, whereas the majority of agents have a few connections only. We generate the network using the preferential attachment algorithm [19]. The probability that an agent has k connections in the network decays as a power law: $P(k) \sim k^{-\alpha}$. The algorithm generates degree distribution with $\alpha = 3$ following empirical estimations [16,29,30]. Comparing our results with Tur *et al.* [10], we use the Watts-Strogatz algorithm [31] that starts with generating a network in which agents are connected to a few nearest neighbors (regular lattice), and rewires every link with a probability μ . As the probability goes to 1, the topology resembles the random network. The so-called small world network topology with still high clustering (similar to regular lattice) but already low enough average path length (similar to random network) is observed for $\mu \in [0.001, 0.1]$ (see Table I). In the following we adopt $\mu = 0.05$.⁶ The networks created with the small world algorithm all have a relatively small degree asymmetry and have been studied without confirmation bias [10].

While the regular lattice and random network are mathematically convenient graphs with little empirical evidence, small world and scale free topologies represent structural properties of networks resulting from physical and digital interactions in the real world. In particular, small world

property is typical for professional networks (movie actors and scientific collaborations [29]) and frequently used to describe interactions leading to the adoption of home-specific goods such as solar PV in [32], while scale free networks are more suited to study information diffusion in online social networks, such as in [17,33]. We also deliberately set the density of the synthetic networks very low (approximately 0.0004), which is in line with empirical estimates by [34].

Figure 2 is meant to illustrate our model of diffusion with social reinforcement with and without the confirmation bias. The top two panels in Fig. 2 exemplify the diffusion processes with and without confirmation bias in a regular lattice with $Q = 0.6$ and $\gamma = 1$. The early adopter E activates her four neighbors $N_E = \{C, D, F, G\}$. Without confirmation bias [Eq. (2)] agent G has minimal quality requirement of $m_{G,1} = 0.60(\frac{1}{4})^1 \leq Q$ and will therefore adopt. Once two connected agents have adopted in a regular lattice, it is an immediate property of Eq. (2) that for $\gamma = 1$ the diffusion will reach 100% for all Q greater than 0.5.

With confirmation bias and $\rho = 2$ [Eq. (3)] the same agent has, in contrast, a minimal quality requirement of $m_{G,1} = 0.60(\frac{e^{-2 \times 0.23}}{e^{-2 \times 0.23} + e^{-2 \times 0.34} + e^{-2 \times 0.14} + e^{-2 \times 0.21}} \times 4)^{-1} \simeq 0.609 \geq Q$ and therefore will not adopt, which prevents the further diffusion process.⁷ This illustrates how under confirmation bias agents become less likely to be influenced by peers with very different preferences.

⁶Reference [10] tested alternative specifications of the parameter but did not find any qualitative difference. We also checked different μ for the small world network in our model with confirmation bias and came to the same conclusion.

⁷For $\rho = 1$ further diffusion would also be prevented as $m_{G,1} = 0.602$, while for $\rho = 3$ its value would have been even larger and equal to 0.618.

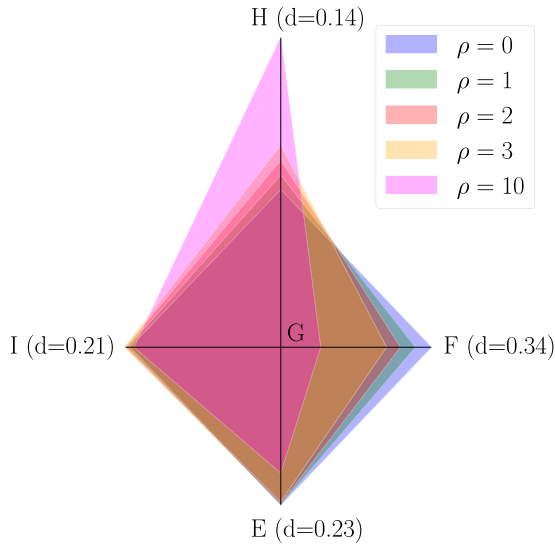


FIG. 3. Relative influence of neighbors on agent G , with different strength of confirmation bias given the distance in preferences (d).

The lower panel in Fig. 2, in contrast, demonstrates that in a network with high degree asymmetry the behavior can spread equally well with and without confirmation bias. This is because applying Eqs. (2) and (3) leads in this example to the same diffusion path with two, three, and four more adopters in subsequent periods.

Figure 3 shows how the relative influence of the neighbors of agent G changes when a confirmation bias is introduced in the model. As noted in Eqs. (7)–(9), when the strength of confirmation bias increases, the most similar (in terms of preferences) neighbor, agent H in this example, has an overarching influence on the decision making of agent G .

To have a more systematic comparison of the four networks for a larger number of adopters and different scenarios of early adopters, as well as alternative distributions of preferences, we proceed with the numerical experiment in the next section.

III. RESULTS

Consistent with [10], we simulate the diffusion process in undirected networks with 10 000 agents with mean degree of 4. The process starts with 10 random early adopters and runs until a steady state is reached, i.e., no new adopter is generated in any subsequent period. As the model can generate different outcomes depending on the initial conditions,⁸ we report average results over 50 restarts for each combination of parameters: quality Q , intensity of social reinforcement γ , distribution of preferences $B(\beta_1, \beta_2)$, and strength of confirmation bias ρ . In Appendix B we also report the period in which the diffusion stops to make the potential trade-off between the rate of adoption (i.e., the share of adopters in the population) and the duration of the diffusion process explicit. We compare the four networks with the two specifications of MQR presented

in Sec. II: without confirmation bias described in Eq. (2) and with confirmation bias from Eq. (3) with $\rho = 2$. This value of ρ corresponds to a moderate confirmation bias (see Fig. 3). In this setting, agents with relatively dissimilar preferences have a lower but still substantial influence on each other. Simulation results for other values of ρ can be found in Appendix A.

In line with the description of our model, the higher quality Q and the intensity of social reinforcement γ consistently contribute to the rising rate of diffusion of behavior all else being equal. While higher Q —capturing higher attractiveness of behavior—simply increases the chance to adopt under the threshold rule in Eq. (1), the higher γ does the same by increasing the role of social reinforcement on potential adopters.

From Fig. 4 we see that without any confirmation bias when the majority of the population has strong preferences against adopting the behavior, the scale free network performs well, reaching a diffusion rate higher or equal to other networks for the majority of combinations of quality and strength of social reinforcement without confirmation bias. The only exception is the intermediate level of quality (0.6–0.8) combined with the high intensity of social interaction ($\gamma \geq 0.6$). Note that in line with our illustration in Fig. 2, 100% diffusion rate in the regular lattice is assured for certain combinations of Q and γ . This result is trivial considering the perfectly structured topology of the regular lattice where any two peers share two more peers in common. According to Eqs. (1) and (2), if $\frac{1}{2\gamma} \leq Q$, then the presence of two connected adopters is a sufficient condition to reach 100% diffusion. One can compare this with the domino chain reaction, where agents cannot resist social pressure from a certain point. In particular, having two connected adopters guarantees a full diffusion for $\gamma = 1$ under $Q \geq 0.5$, for $\gamma = 0.8$ under $Q \geq 0.575$, $\gamma = 0.6$ under $Q \geq 0.66$, $\gamma = 0.4$ under $Q \geq 0.758$, etc.

Once we introduce the confirmation bias in Fig. 5, we observe a deterioration of the rate of diffusion in the regular lattice while performance of all other networks, particularly the scale free one, remains remarkably robust. This is made clear by Fig. 6, which shows the change in adoption rate when confirmation bias is introduced. This deterioration happens because the bias raises the propensity of agents to resist social pressure from peers with relatively different preferences. Hence the “domino effect” described in the regular lattice under no confirmation bias arises only for much higher values of Q . For larger ρ , there is no threshold quality such that 100% diffusion rate in the regular lattice is guaranteed (see Figs. 8 and 9 in Appendix A). Combined with the fact that a few resisting agents are sufficient to isolate a large share of the network from early adopters (Fig. 2), we observe the very high “fragility” of the performance of the highly clustered network towards the presence of the confirmation bias. It is worth mentioning that already a few short path links present in the small world network solve the problem and make the network robust to the bias. Thanks to those links, agents bypass the resisting nodes and effectively prevent them from stopping further diffusion. Increasing further the number of adopters later can convert the resisting agent into an adopter anyway.

To check the robustness of this result, we explore alternative values of the confirmation bias strength ρ (see Appendix A). We find that the performance of the regular lattice deteriorates even further when the similarity in

⁸Three features subject to random number initialization influence the outcome: the draw of individual switching costs, the choice of early adopters, and the topology of the network.

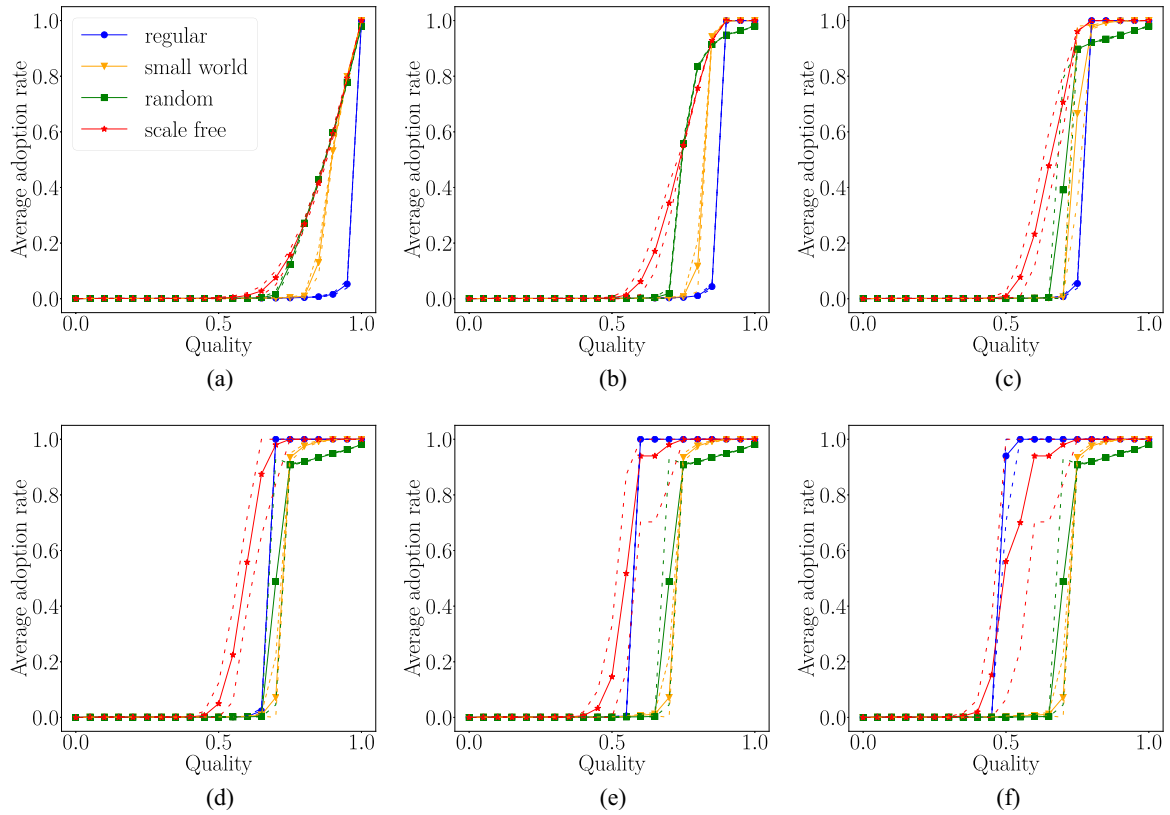


FIG. 4. Adoption rate without confirmation bias, $\rho = 0$, and for $\pi \sim B(4, 1)$ with social reinforcement intensity (a) $\gamma = 0$, (b) $\gamma = 0.2$, (c) $\gamma = 0.4$, (d) $\gamma = 0.6$, (e) $\gamma = 0.8$, and (f) $\gamma = 1$. *Note.* The dashed lines represent two standard deviations around the average.

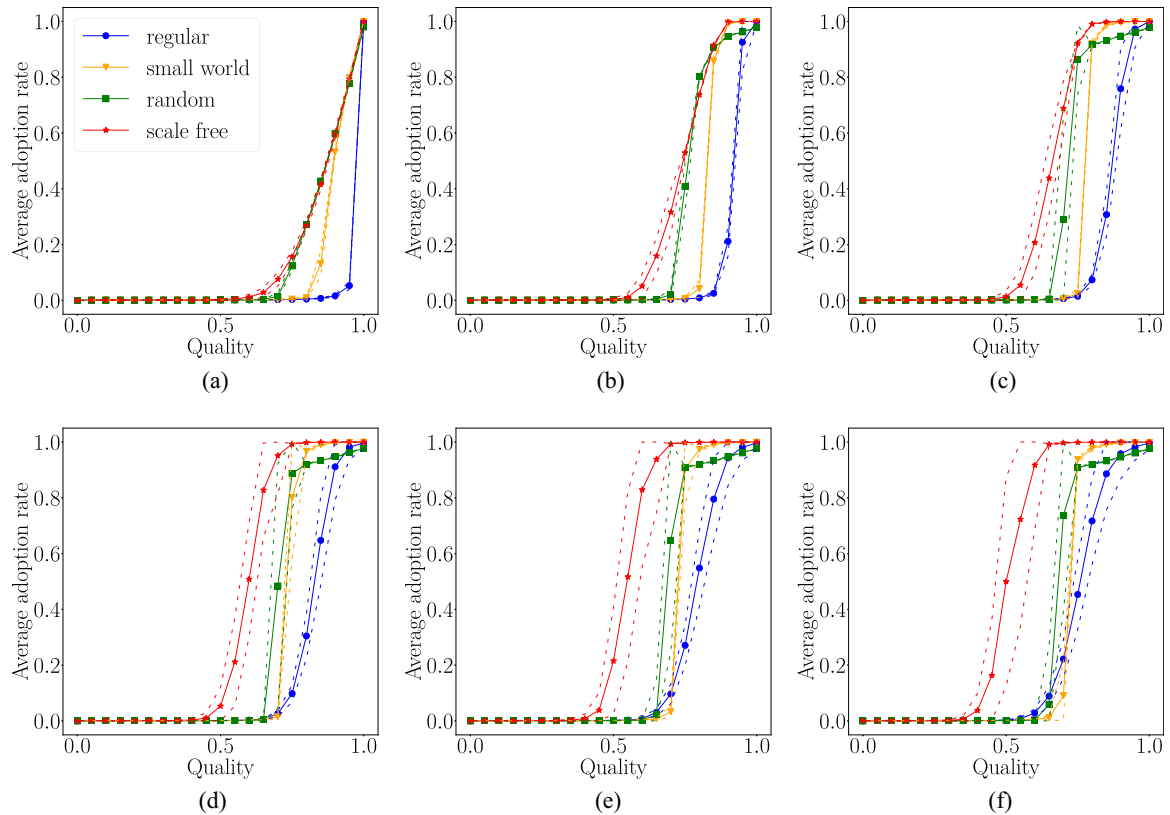


FIG. 5. Adoption rate with confirmation bias, $\rho = 2$, and for $\pi \sim B(4, 1)$ with social reinforcement intensity (a) $\gamma = 0$, (b) $\gamma = 0.2$, (c) $\gamma = 0.4$, (d) $\gamma = 0.6$, (e) $\gamma = 0.8$, and (f) $\gamma = 1$. *Note.* The dashed lines represent two standard deviations around the average.

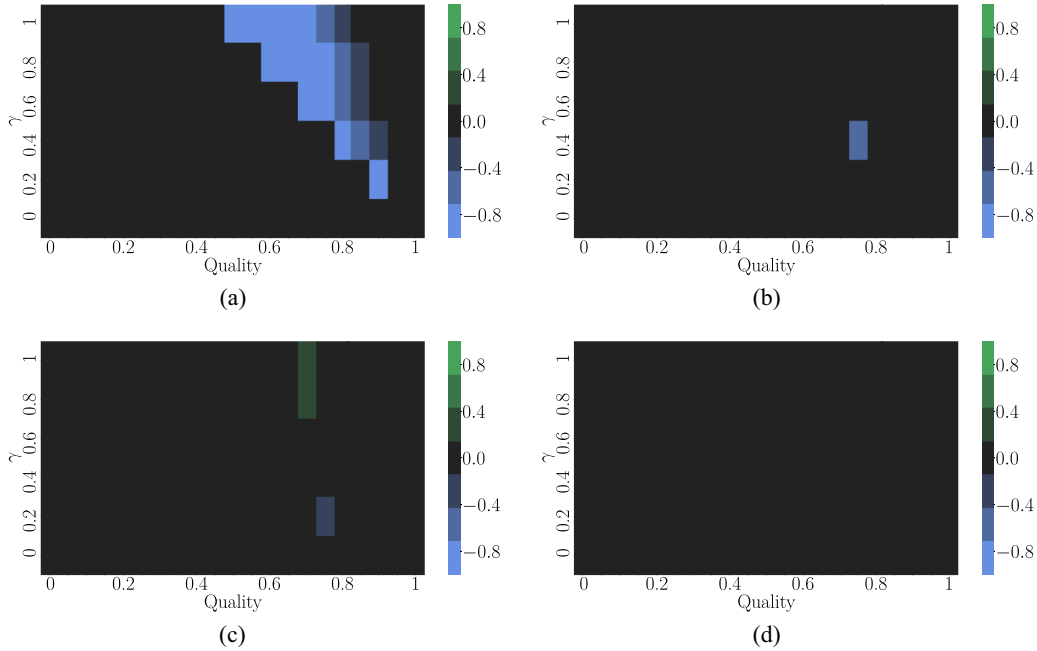


FIG. 6. Difference in percentage points between the adoption rate with confirmation bias, $\rho = 2$, and without confirmation bias, $\rho = 0$, for $\pi \sim B(4, 1)$ (a) regular, (b) small world, (c) random, and (d) scale free. *Note.* Negative values mean that the adoption rate is lower under confirmation bias. The results are generated for different combinations of quality and intensity of social reinforcement (γ).

preferences plays a stronger role in the diffusion process. For higher value of ρ , we find that the adoption rate in the regular lattice is close to zero for virtually all combinations of parameters. This confirms that the diffusion process in clustered networks is highly contingent on the weight agents assigned to similar peers.

Another important consequence of the introduction of the confirmation bias is the fact that the scale free network becomes the best performing graph in terms of diffusion for virtually all combinations of quality and strength of social interaction (Fig. 5). Thus, unlike previous studies, we find that high clustering is not necessary to reach high diffusion rates when the majority of agents originally resists the adoption. The most connected agents in the scale free network act like “influence hubs”: they are more likely to have early adopters among neighbors (hence adopt the behavior themselves), and subsequently distribute the signal to their numerous peers quickly increasing the strength of social pressure on other agents. Unlike clustering, this structural property is not sensitive to the introduction of weighted interactions. Although describing the important role of “influence hubs” is not novel in the case of simple diffusion, the presence of high degree asymmetry allows for a broad and fast diffusion under social reinforcement even with a low clustering and confirmation bias.

Comparing diffusion across networks in terms of speed (number of periods until diffusion stops) supports the advantage of the scale free network. Thus it does not only reach highest diffusion rates, but does so in the shortest number of periods (see Appendix B). The latter is important if one is concerned not just with the final outcome but also the speed of its realization. A good example can again be environmental behavior: a quick diffusion would help to reduce CO₂ emissions early enough to prevent global warming of 1.5 °C above preindustrial levels [35]. Other network topologies, whenever

they reach relatively high diffusion rates, take much more time. This is particular true for the regular lattice. Taking its very long average path length (Table I), however, this is not surprising.⁹

We also test the model under alternative distributions of preferences like the uniform distribution or majority of agents having low switching costs (see Appendix C). In those cases the scale free network does not always rank first, but is only slightly inferior to the best performing network.

IV. CONCLUSION

The mounting empirical evidence on the role of social interaction in affecting individual decision making and behavior spreading has drawn attention to the search of network topology that best promotes the diffusion process, both in terms of adoption rate and the amount of time needed. Earlier, the literature demonstrated that clustered networks best foster diffusion if a majority of agents is resistant to adopt. This is because the seemingly redundant ties reinforce the probability of adoption of the most resisting agents. If, in contrast, agents are open to adopting new behavior, networks with shortest paths are good enough to reach high diffusion rates within a short amount of time.

⁹Note that the curves of diffusion times for different Q resemble an inverted U shape. This is because for greater Q agents are more likely to adopt without any social reinforcement. In fact, for $Q \rightarrow 1$ any agent adopts once he has one peer among adopters. Hence the speed of diffusion for $Q \rightarrow 1$ is increasing. Low diffusion time for $Q \rightarrow 0$, in turn, is due to the low diffusion rates where behavior spreading stops early in time.

The present paper makes the setting studied by [10] more realistic by differentiating the influence of peers on the agent’s decision to adopt depending on the distance in their preferences. In doing so, we follow the experimental evidence that people put a higher weight on opinions that conform to their beliefs—the so-called confirmation bias. Furthermore, accepting the growing role of online social networks and their highly asymmetric degree distribution exhibiting power law, we add the scale free topology in our network comparison.

We demonstrate that the introduction of the bias changes the ranking of networks in terms of the diffusion rates they achieve. In particular, while the regular lattice was performing best when the majority of agents have a strong preference against adopting the behavior, it becomes last once agents start differentiating their neighbors based on the distance in their preferences and, consequently, resist the adoption. Such a fragility is due to the absence of short paths between agents allowing one to bypass the resisting nodes. In contrast, other studied networks, and particularly the scale free one, are robust to the introduction of this assumption to the model. The scale free network becomes the best performing one under such a setting in terms of diffusion for different intensities of social reinforcement. Unlike the existing literature, we find

that high clustering is not necessary to explain high diffusion rates when the majority of agents is reluctant to adopt. This is because high degree nodes serve as influence hubs collecting and redistributing the signal of a new behavior raising social pressure in the network. Thus our results shift the focus from network clustering to network degree distribution as the key factor for diffusion. As highly asymmetric networks are pervasive in digital social platforms, our results suggest that a diffusion will be more effective in those platforms than in spatial offline networks characterized by higher clustering and lower degree asymmetry.

ACKNOWLEDGMENTS

This work was supported by an ERC Advanced Grant under the European Union’s Horizon 2020 research and innovation program (Grant No. 741087). I.S. acknowledges financial support from the Russian Science Foundation (RSF Grant No. 19-18-00262). We have greatly benefited from discussions with Jeroen van den Bergh, Elena Tur, Paolo Zeppini, and two anonymous referees. All remaining shortcomings are solely our responsibility.

APPENDIX A: RESULTS WITH DIFFERENT CONFIRMATION BIAS PARAMETERS

As the confirmation bias plays a stronger role in the diffusion process, the performance of the regular network decreases (see Figs. 7–9). The introduction of a strong confirmation bias ($\rho = 10$) has a larger negative impact on the diffusion in the more clustered networks, namely the regular lattice and small world networks (see Fig. 10).

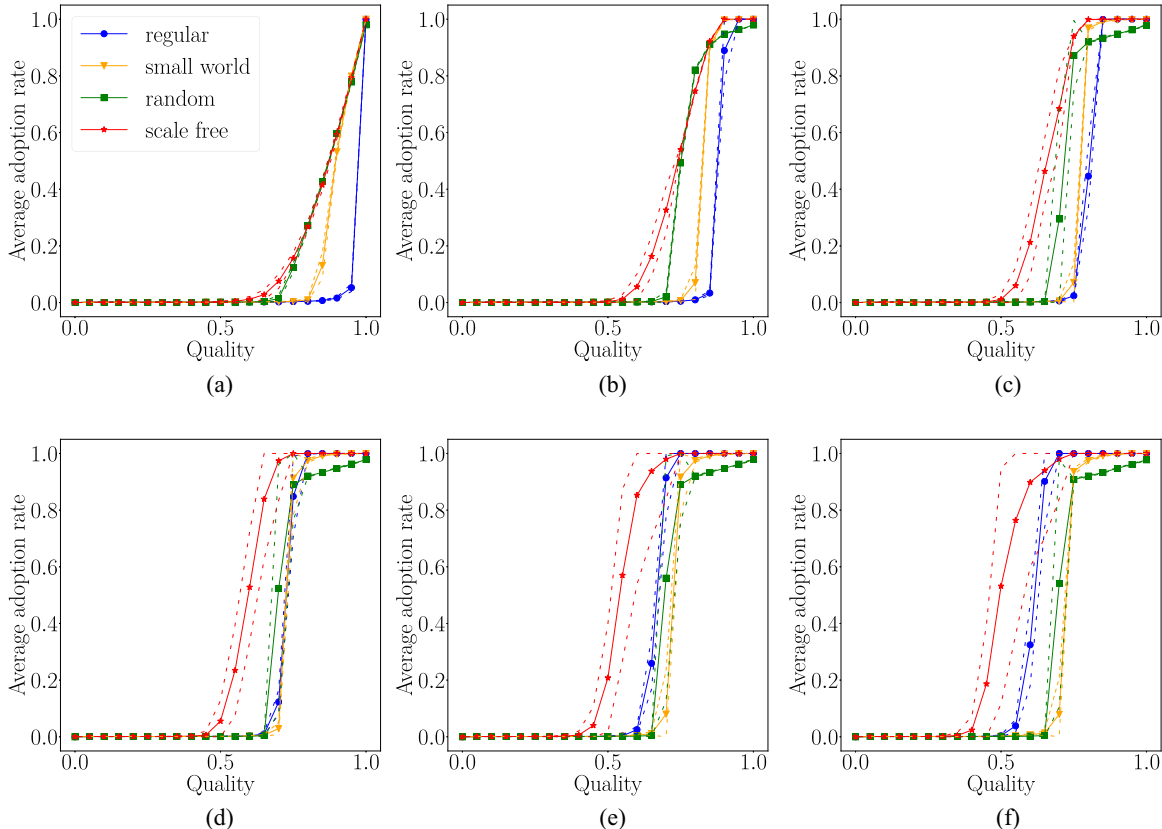


FIG. 7. Adoption rate with confirmation bias, $\rho = 1$, and for $\pi \sim B(4, 1)$ with social reinforcement intensity (a) $\gamma = 0$, (b) $\gamma = 0.2$, (c) $\gamma = 0.4$, (d) $\gamma = 0.6$, (e) $\gamma = 0.8$, and (f) $\gamma = 1$. Note. The dashed lines represent two standard deviations around the average.

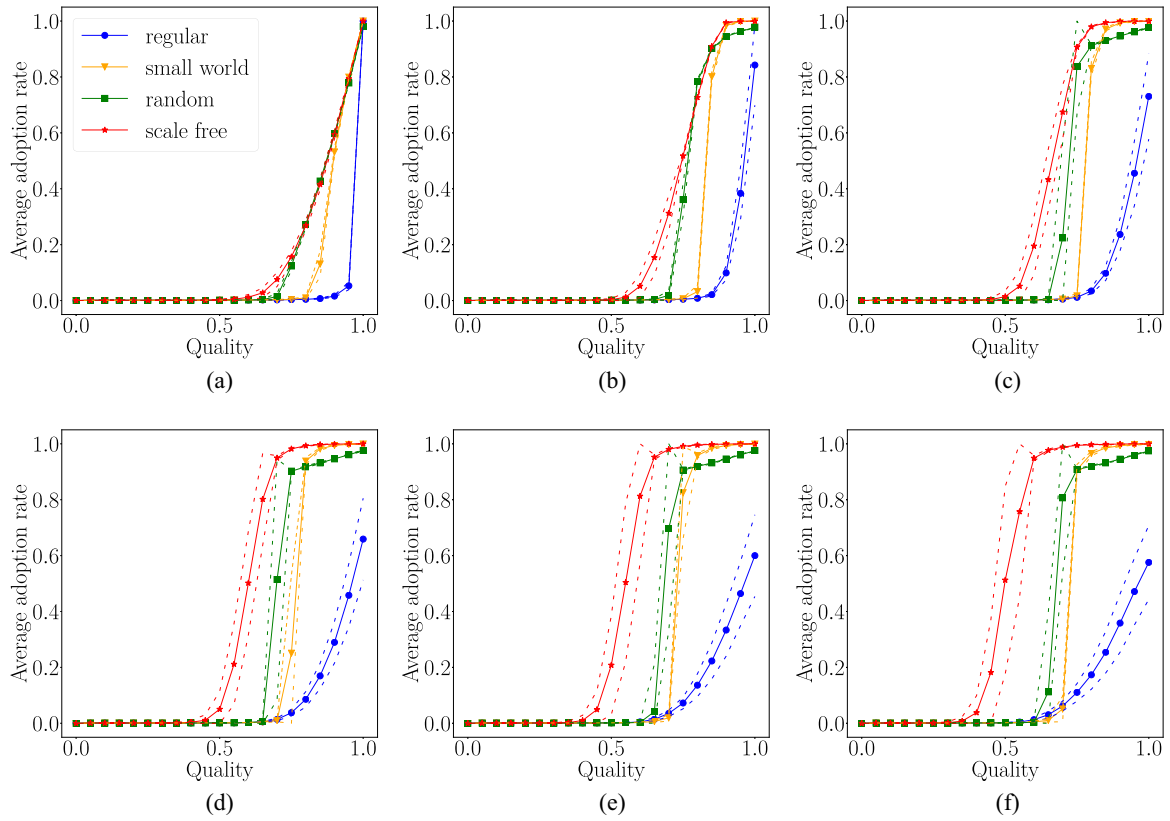


FIG. 8. Adoption rate with confirmation bias, $\rho = 3$, and for $\pi \sim B(4, 1)$ with social reinforcement intensity (a) $\gamma = 0$, (b) $\gamma = 0.2$, (c) $\gamma = 0.4$, (d) $\gamma = 0.6$, (e) $\gamma = 0.8$, and (f) $\gamma = 1$. *Note.* The dashed lines represent two standard deviations around the average.

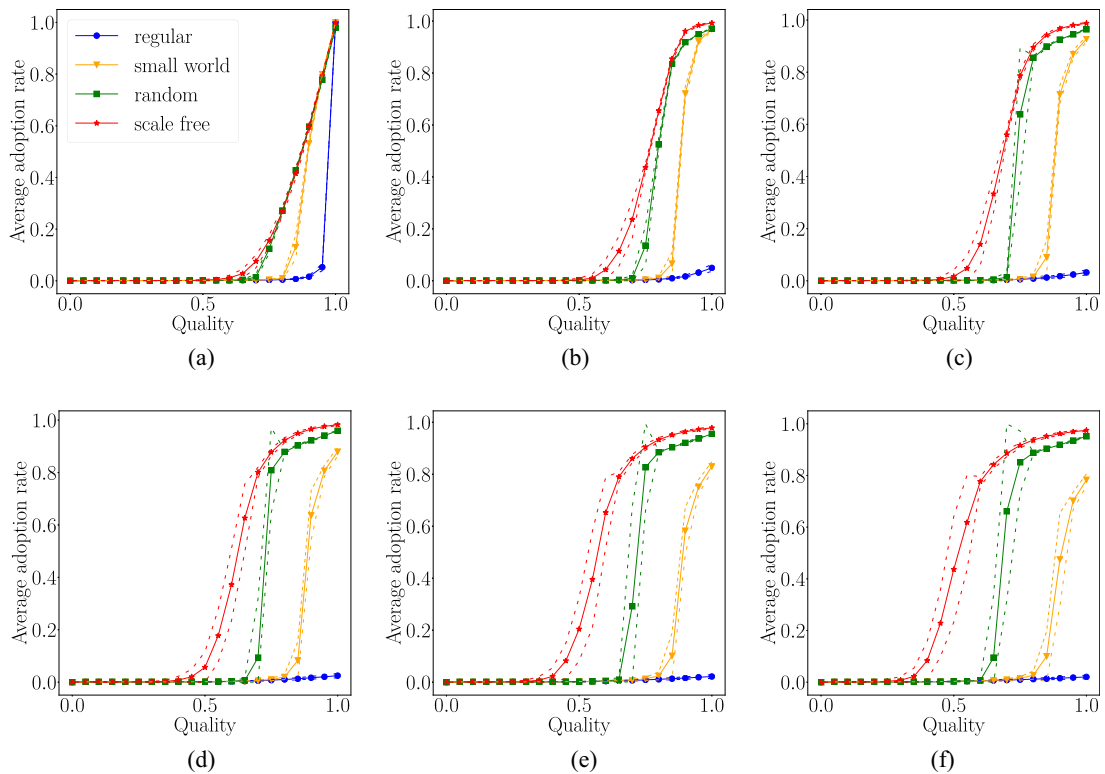


FIG. 9. Adoption rate with confirmation bias, $\rho = 10$, and for $\pi \sim B(4, 1)$ with social reinforcement intensity (a) $\gamma = 0$, (b) $\gamma = 0.2$, (c) $\gamma = 0.4$, (d) $\gamma = 0.6$, (e) $\gamma = 0.8$, and (f) $\gamma = 1$. *Note.* The dashed lines represent two standard deviations around the average.

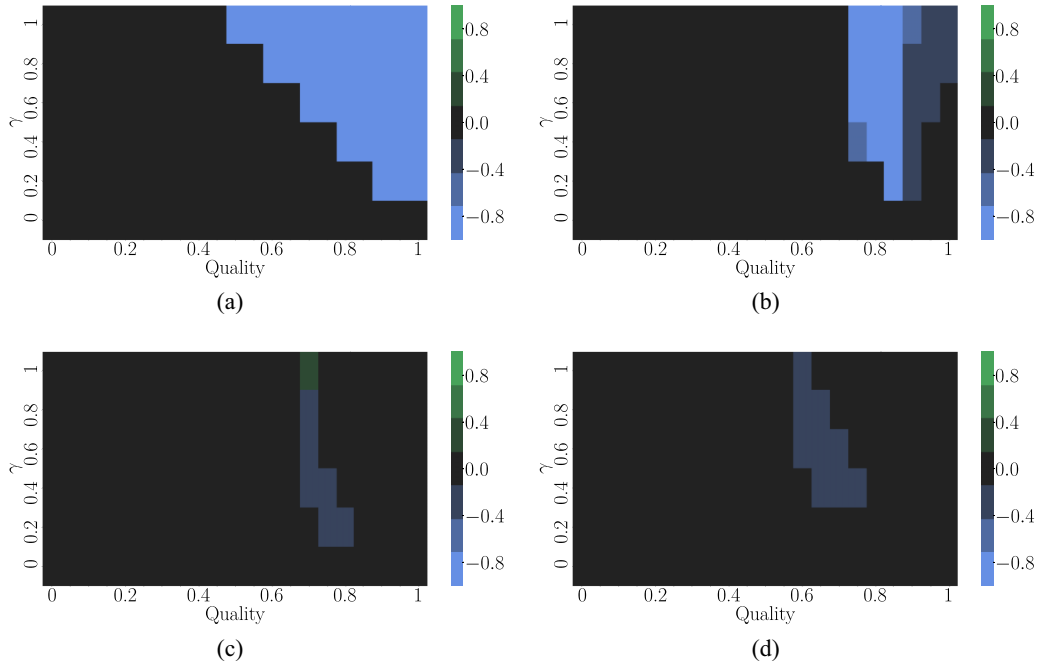


FIG. 10. Difference in percentage points between the adoption rate with confirmation bias, $\rho = 10$, and without confirmation bias, $\rho = 0$, for $\pi \sim B(4, 1)$ (a) regular, (b) small world, (c) random, and (d) scale free. *Note.* Negative values mean that the adoption rate is lower under confirmation bias. The results are generated for different combinations of quality and intensity of social reinforcement (γ).

APPENDIX B: TIME OF DIFFUSION

The scale free network consistently reaches a maximum diffusion with the shortest number of periods (see Figs. 11 and 12). In the cases for which the regular lattice outperforms the scale free network ($\rho = 0$ and $\gamma \geq 0.8$), the diffusion time necessary is higher by several orders of magnitude (see Fig. 11).

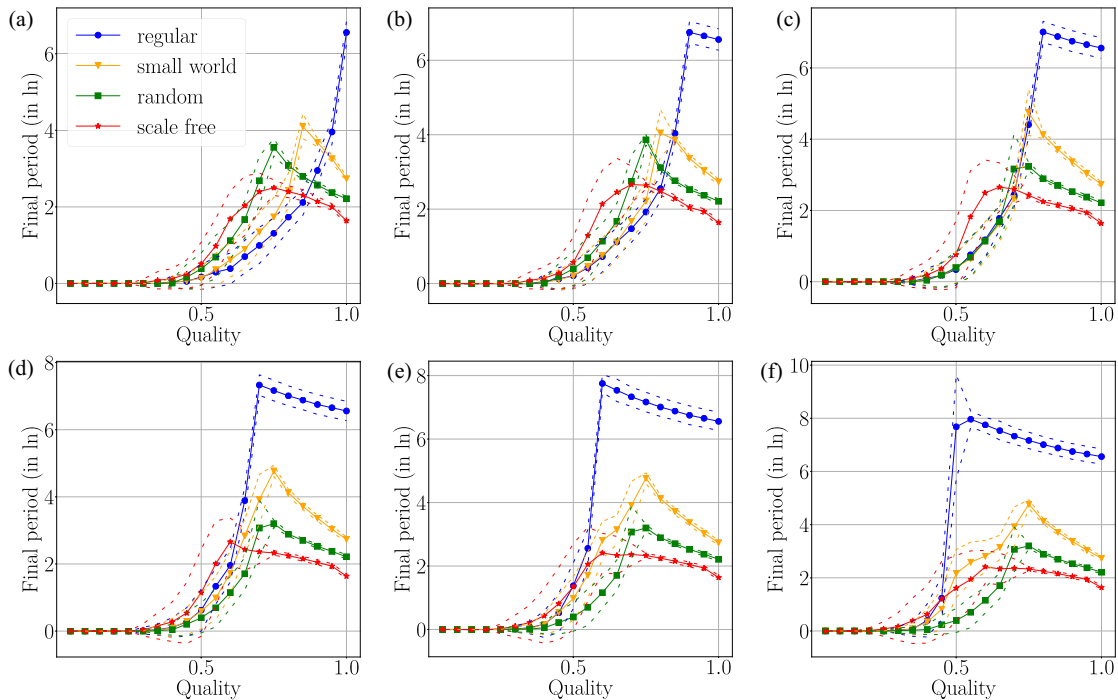


FIG. 11. Diffusion time without confirmation bias, $\rho = 0$, and for $\pi \sim B(4, 1)$ with social reinforcement intensity (a) $\gamma = 0$, (b) $\gamma = 0.2$, (c) $\gamma = 0.4$, (d) $\gamma = 0.6$, (e) $\gamma = 0.8$, and (f) $\gamma = 1$. *Note.* The dashed lines represent two standard deviations around the average.

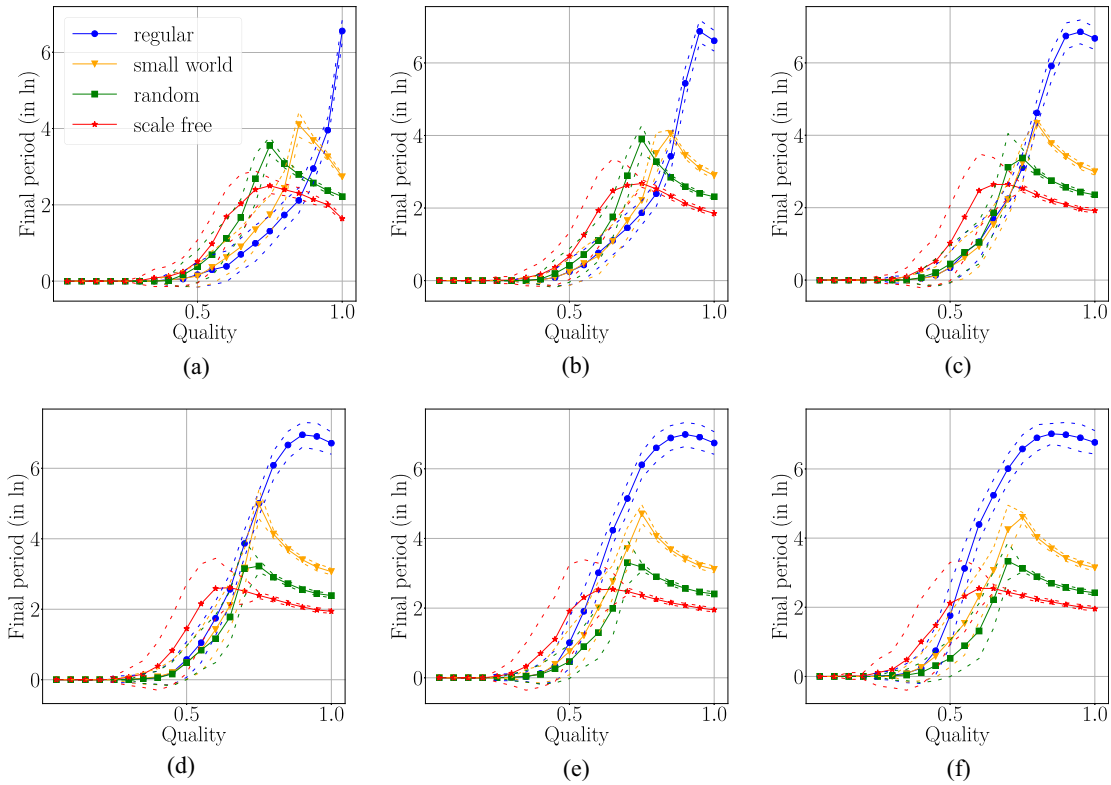


FIG. 12. Diffusion time with confirmation bias, $\rho = 2$, and for $\pi \sim B(4, 1)$ with social reinforcement intensity (a) $\gamma = 0$, (b) $\gamma = 0.2$, (c) $\gamma = 0.4$, (d) $\gamma = 0.6$, (e) $\gamma = 0.8$, and (f) $\gamma = 1$. *Note.* The dashed lines represent two standard deviations around the average.

APPENDIX C: DIFFERENT SWITCHING COSTS DISTRIBUTIONS

Under alternative distributions of switching costs, the scale free network ranks first for a vast majority of social reinforcement intensity and confirmation bias combinations (see Figs. 13–18).

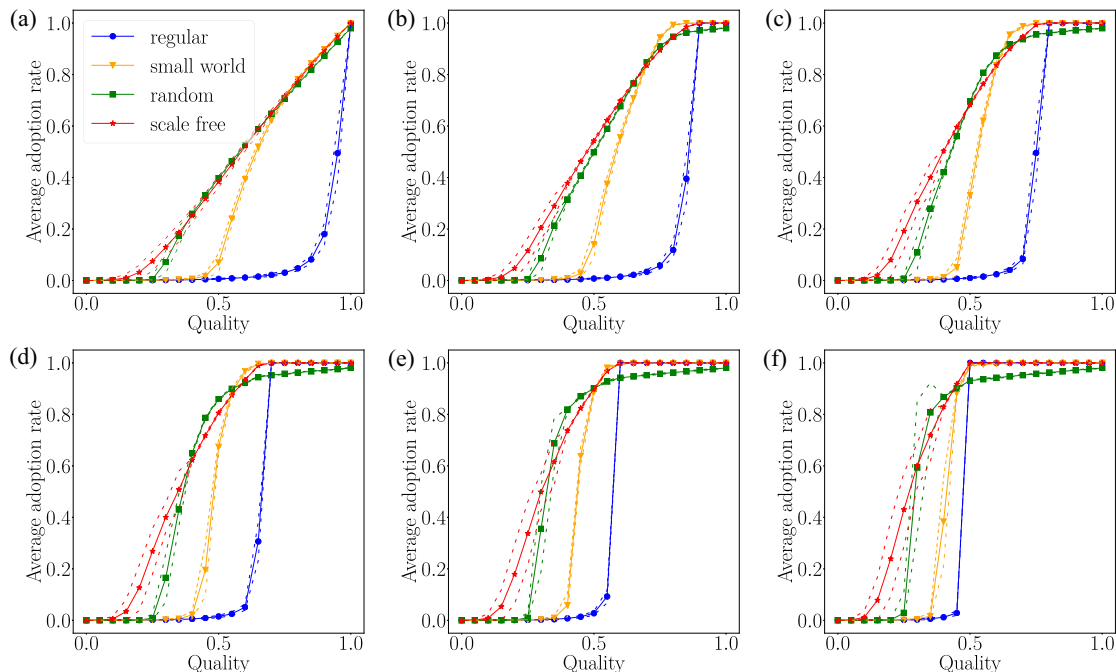


FIG. 13. Adoption rate with confirmation bias, $\rho = 0$, and for $\pi \sim B(1, 1)$ with social reinforcement intensity (a) $\gamma = 0$, (b) $\gamma = 0.2$, (c) $\gamma = 0.4$, (d) $\gamma = 0.6$, (e) $\gamma = 0.8$, and (f) $\gamma = 1$. *Note.* The dashed lines represent two standard deviations around the average.

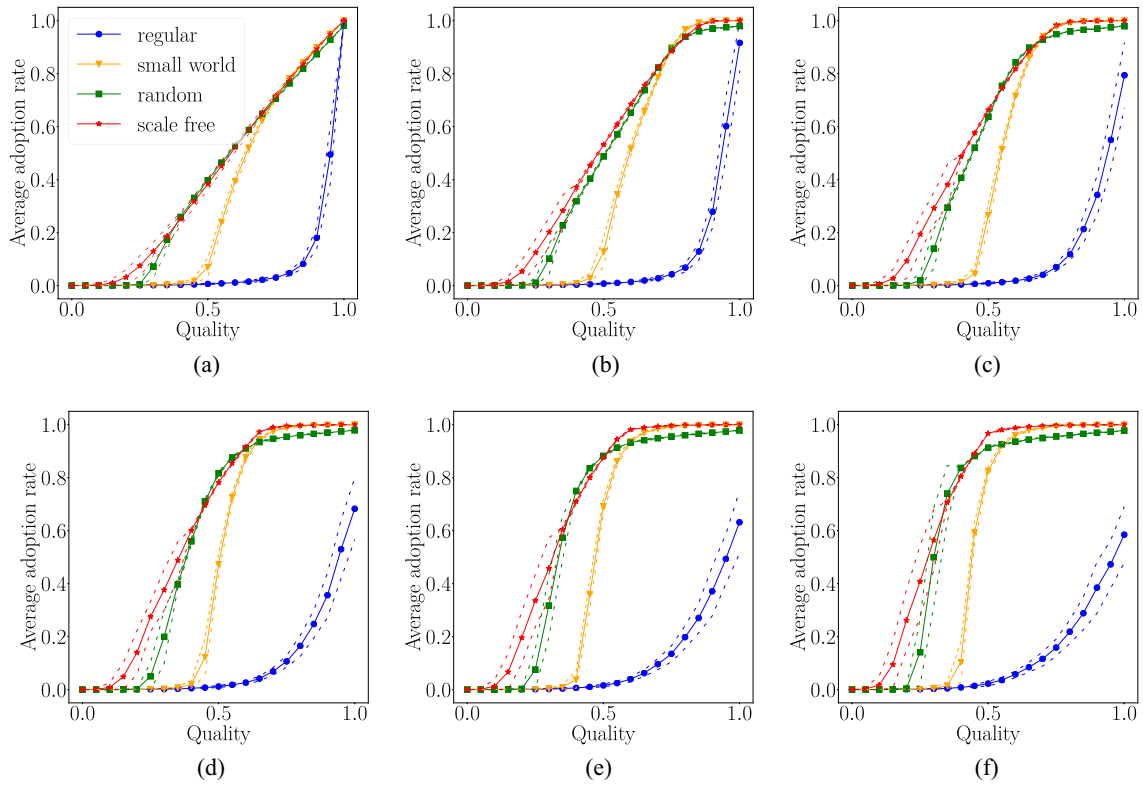


FIG. 14. Adoption rate with confirmation bias, $\rho = 2$, and for $\pi \sim B(1, 1)$ with social reinforcement intensity (a) $\gamma = 0$, (b) $\gamma = 0.2$, (c) $\gamma = 0.4$, (d) $\gamma = 0.6$, (e) $\gamma = 0.8$, and (f) $\gamma = 1$. *Note.* The dashed lines represent two standard deviations around the average.

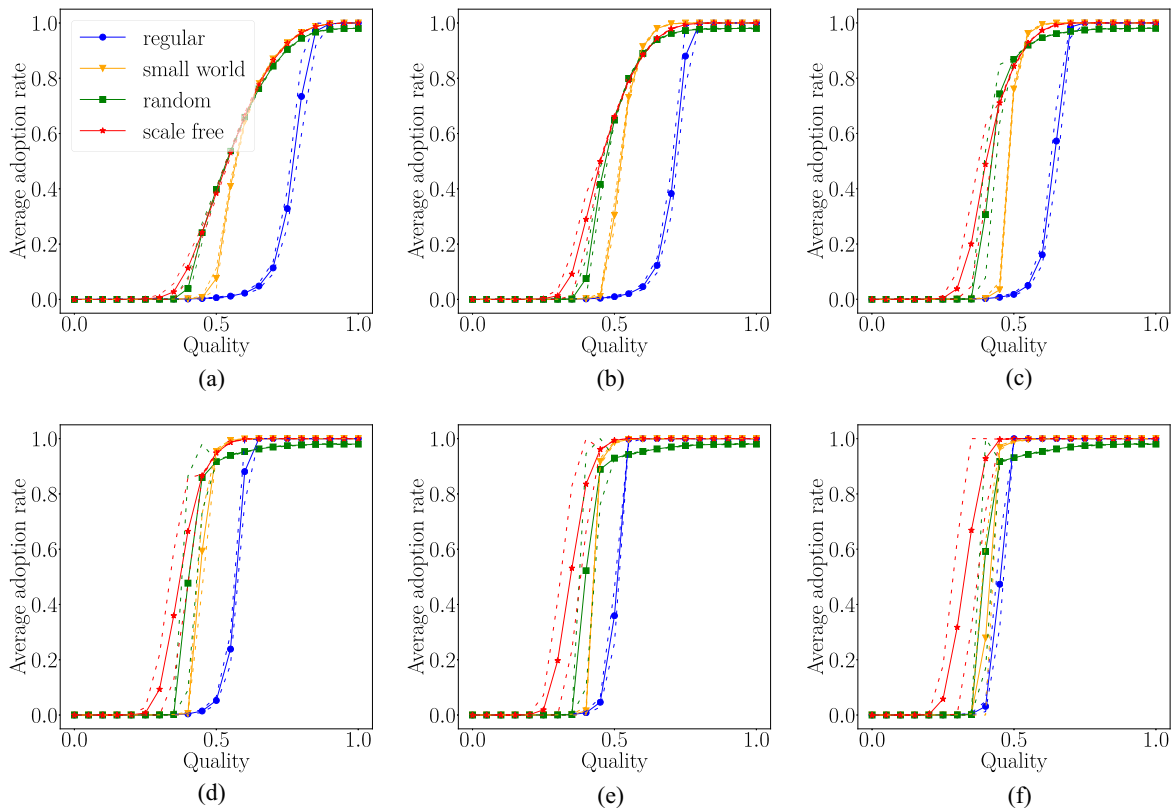


FIG. 15. Adoption rate without confirmation bias, $\rho = 0$, and for $\pi \sim B(4, 4)$ with social reinforcement intensity (a) $\gamma = 0$, (b) $\gamma = 0.2$, (c) $\gamma = 0.4$, (d) $\gamma = 0.6$, (e) $\gamma = 0.8$, and (f) $\gamma = 1$. *Note.* The dashed lines represent two standard deviations around the average.

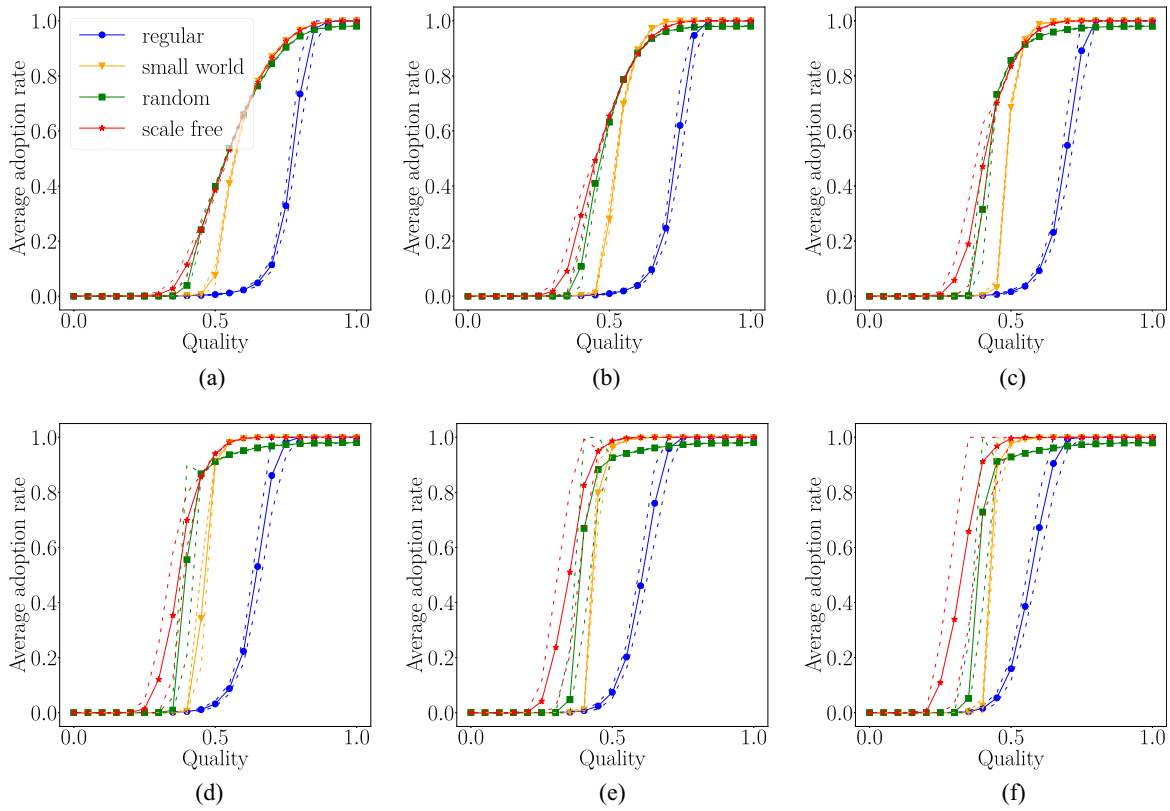


FIG. 16. Adoption rate with confirmation bias, $\rho = 2$, and for $\pi \sim B(4, 4)$ with social reinforcement intensity (a) $\gamma = 0$, (b) $\gamma = 0.2$, (c) $\gamma = 0.4$, (d) $\gamma = 0.6$, (e) $\gamma = 0.8$, and (f) $\gamma = 1$. *Note.* The dashed lines represent two standard deviations around the average.

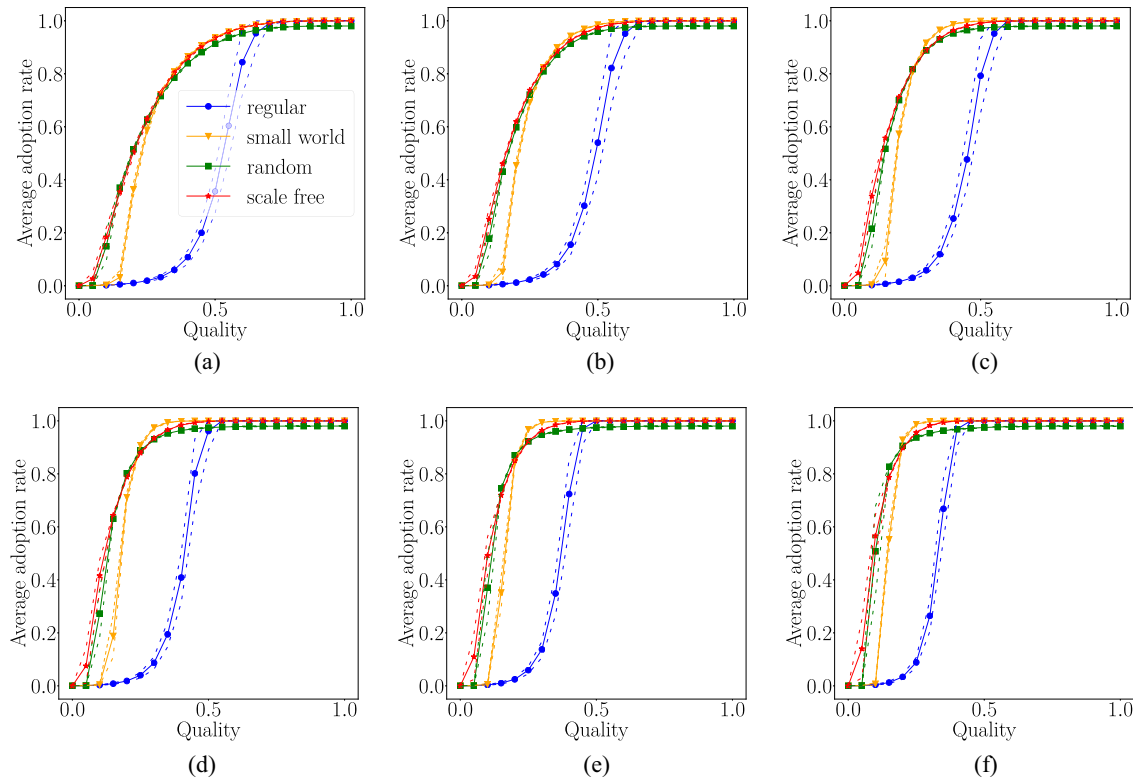


FIG. 17. Adoption rate with confirmation bias, $\rho = 0$, and for $\pi \sim B(1, 4)$ with social reinforcement intensity (a) $\gamma = 0$, (b) $\gamma = 0.2$, (c) $\gamma = 0.4$, (d) $\gamma = 0.6$, (e) $\gamma = 0.8$, and (f) $\gamma = 1$. *Note.* The dashed lines represent two standard deviations around the average.

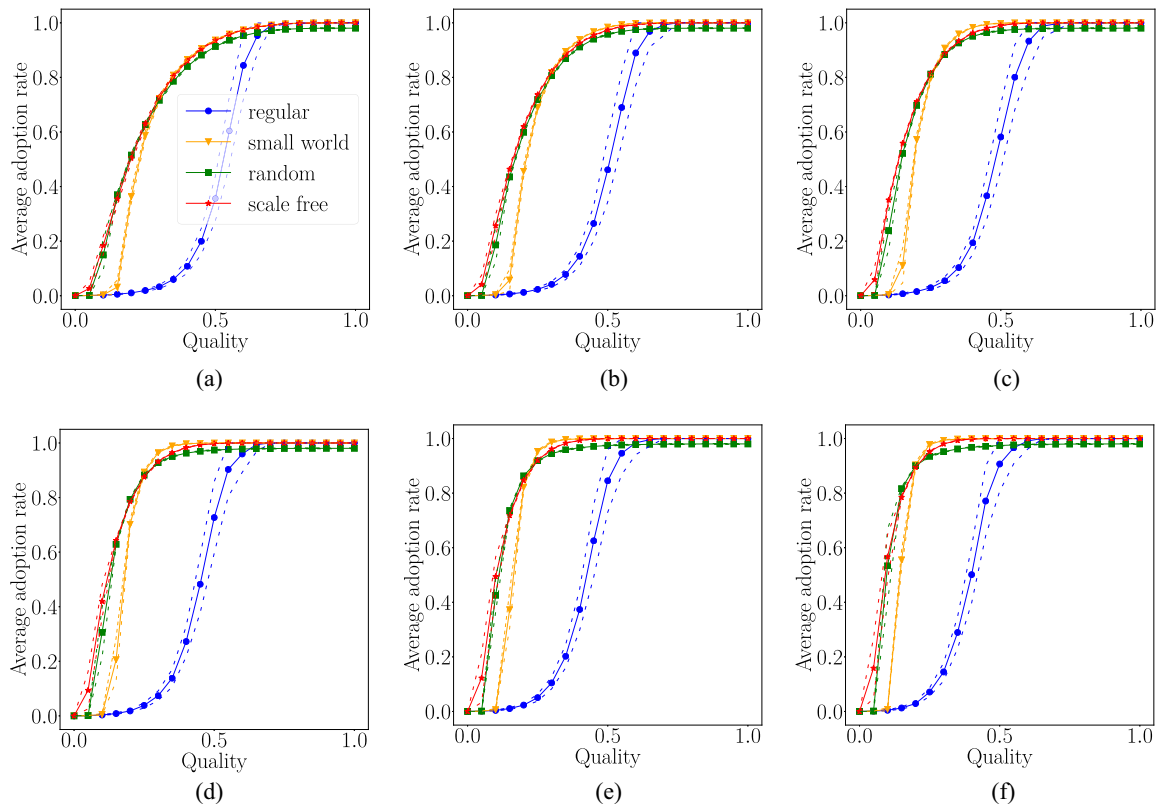


FIG. 18. Adoption rate with confirmation bias, $\rho = 2$, and for $\pi \sim B(1, 4)$ with social reinforcement intensity (a) $\gamma = 0$, (b) $\gamma = 0.2$, (c) $\gamma = 0.4$, (d) $\gamma = 0.6$, (e) $\gamma = 0.8$, and (f) $\gamma = 1$. *Note.* The dashed lines represent two standard deviations around the average.

-
- [1] H. Allcott, *J. Pub. Econ.* **95**, 1082 (2011).
- [2] W. Abrahamse and L. Steg, *Glob. Environ. Change* **23**, 1773 (2013).
- [3] B. Bollinger and K. Gillingham, *Market. Sci.* **31**, 900 (2012).
- [4] Z. Babutsidze and A. Chai, *Ecol. Econ.* **146**, 290 (2018).
- [5] R. B. Cialdini, *Curr. Direct. Psychol. Sci.* **12**, 105 (2003).
- [6] S. A. Delre, W. Jager, and M. A. Janssen, *Comput. Math. Org. Theory* **13**, 185 (2007).
- [7] D. Centola, *Science* **329**, 1194 (2010).
- [8] A. Nematzadeh, E. Ferrara, A. Flammini, and Y.-Y. Ahn, *Phys. Rev. Lett.* **113**, 088701 (2014).
- [9] M. Zheng, L. Lu, and M. Zhao, *Phys. Rev. E* **88**, 012818 (2013).
- [10] E. M. Tur, P. Zeppini, and K. Frenken, *Phys. Rev. E* **97**, 022302 (2018).
- [11] S. E. Asch, *Sci. Am.* **193**, 31 (1955).
- [12] C. G. Lord, L. Ross, and M. R. Lepper, *J. Person. Soc. Psychol.* **37**, 2098 (1979).
- [13] R. Nickerson, *Rev. Gen. Psychol.* **2**, 175 (1998).
- [14] R. B. Cialdini and N. J. Goldstein, *Ann. Rev. Psychol.* **55**, 591 (2004).
- [15] P. J. Silvia, *Basic Appl. Soc. Psychol.* **27**, 277 (2005).
- [16] A. Mislove, M. Marcon, K. P. Gummadi, P. Druschel, and B. Bhattacharjee, in *Proceedings of the 7th ACM SIGCOMM Conference on Internet Measurement, IMC '07* (ACM Press, New York, 2007), pp. 29–42.
- [17] Z. Babutsidze and M. Valente, *Indust. Corp. Change* **28**, 459 (2019).
- [18] E. Bakshy, I. Rosenn, C. Marlow, and L. Adamic, The role of social networks in information diffusion, in *Proceedings of the 21st International Conference on World Wide Web* (ACM Press, New York, 2012), pp. 519–528.
- [19] A.-L. Barabási and R. Albert, *Science* **286**, 509 (1999).
- [20] R. Pastor-Satorras and A. Vespignani, *Phys. Rev. Lett.* **86**, 3200 (2001).
- [21] P. Zeppini and K. Frenken, *J. Artif. Societ. Soc. Simul.* **21**, 1 (2018).
- [22] S. Cantono and G. Silverberg, *Technol. Forecast. Soc. Change* **76**, 487 (2009).
- [23] G. Deffuant, D. Neau, F. Amblard, and G. Weisbuch, *Adv. Complex Syst.* **03**, 87 (2000).
- [24] J. Lorenz, *Complexity* **15**, 43 (2010).
- [25] A. Das, S. Gollapudi, and K. Munagala, in *Proceedings of the 7th ACM International Conference on Web Search and Data Mining, WSDM '14* (ACM Press, New York, 2014), pp. 403–412.
- [26] G. Weisbuch, G. Deffuant, F. Amblard, and J.-P. Nadal, *Complexity* **7**, 55 (2002).
- [27] R. Hegselmann and U. Krause, *J. Artif. Societ. Soc. Simul.* **5** (2002).
- [28] Z. Babutsidze and R. Cowan, *J. Econ. Interact. Coord.* **9**, 151 (2014).

- [29] R. Albert and A.-L. Barabási, *Rev. Mod. Phys.* **74**, 47 (2002).
- [30] M. De Domenico, A. Lima, P. Mougel, and M. Musolesi, *Sci. Rep.* **3**, 2980 (2013).
- [31] D. J. Watts and S. H. Strogatz, *Nature (London)* **393**, 440 (1998).
- [32] V. Rai and S. A. Robinson, *Environ. Model. Softw.* **70**, 163 (2015).
- [33] M. J. Eppstein, D. K. Grover, J. S. Marshall, and D. M. Rizzo, *Energy Policy* **39**, 3789 (2011).
- [34] H. Hu and X. Wang, *Phys. Lett. A* **373**, 1105 (2009).
- [35] IPCC, SR1.5: Global Warming of 1.5 °C—Chapter 4: Strengthening and implementing the global response, <http://www.ipcc.ch/report/sr15/>.